Supporting Information

A homoleptic rare-earth-metal tetramethylindate

Philipp Wetzel,[a] Cäcilia Maichle-Mössmer,[a] and Reiner Anwander[a,*]

[a] Institut für Anorganische Chemie, Eberhardt Karls Universität Tübingen, Auf der Morgenstelle 18, D-72076 Tübingen, Germany. E-Mail: reiner.anwander@uni-tuebingen.de

Table of Contents

Experimental

General Considerations

All manipulations were carried out under rigorous exclusion of air and moisture, using standard Schlenk and glovebox techniques (MBraun MB200B <1 ppm O_2, <1 ppm H_2O, argon atmosphere). All solvents were supplied by Merck KGaA, purified using a SPS solvent purification system (MBraun) and stored inside a glovebox. Tetrahydrofuran was additionally dried over molecular sieves (3 Å). Benzene-d_6, toluene-d_8 and THF-d_8 were obtained by Merck KGaA. THF-d_8 was dried over molecular sieves (3 Å). Trimethylindium and 1,4,7-trimethyl-1,4,7-triazacyclononane (Me_3TACN) were purchased from abcr GmbH and used without further purification. Argon was supplied by Westfalen AG. Homoleptic La($AlMe_4$)$_3$, Ce($AlMe_4$)$_3$ and Nd($AlMe_4$)$_3$ were prepared according to standard literature procedures.[1] Chemicals were stored at –40 °C. NMR spectra of air and moisture sensitive compounds were recorded using J. Young-valved NMR tubes on a Bruker AVII+400 (^{1}H: 400.11 MHz; ^{13}C: 100.61 MHz) and a Bruker AVII+500 spectrometer (^{1}H: 500.13 MHz; ^{13}C: 125.76 MHz). NMR chemical shifts are referenced to solvent residual resonances and reported in parts per million, relative to tetramethylsilane. IR spectra were recorded on a NICOLET 6700 FTIR spectrometer (Thermo Fisher Scientific) by using a DRIFT chamber with dry KBr/sample mixtures and KBr windows. Elemental analyses were performed on an Elementar Vario MICRO Cube. It is very important to note that the homoleptic complexes Ln($InMe_4$)$_3$ readily start to decompose at ambient temperature. For performing the elemental analysis, extremely rapid handling of the crystalline material was required which also excluded drying of the crystalline material. Therefore, any analysis is also skewed by the presence of solvent. The analysis of the cluster compounds was performed with the crude reaction products, which are composed of mixtures of cluster compounds. Aluminium and indium contents were determined *via* ICP-OES on a Thermo Scientific iCAP 7000 Series.

Caution! Note that organoaluminum as well as organoindium compounds react violently with air and moisture and may explode in water.

Procedures

La($InMe_4$)$_3$ (3)

Route a): A solution of La($AlMe_4$)$_3$ (209 mg, 0.522 mmol, 1 equiv.) in *n*-hexane (8 mL) was cooled to 0 °C. Subsequently, $InMe_3$ (334 mg, 2.09 mmol, 4 equiv.) dissolved in *n*-hexane (2 mL) and THF (0.07 mL; 0.78 mmol; 1.5 equiv.) were added at 0 °C. After vigorous stirring for 20 minutes, THF (0.09 mL; 0.99 mmol; 1.9 equiv.) was added to the solution over 1 hour. Following additional stirring for 40 minutes, toluene (2 mL) was added, and the resulting solution was concentrated *in vacuo* and stored at –40 °C. Crystallization afforded 273 mg (0.412 mmol, 79 %) colourless crystals of La($InMe_4$)$_3$. ^{1}H NMR (500.1 MHz, toluene-d_8, 0 °C): δ = -0.07 (s, 36H, CH_3) ppm. ^{13}C NMR

(125.8 MHz, toluene-d_8, 0 °C): δ = 5.01 (CH$_3$) ppm. DRIFT (KBr, cm^{-1}): 3017 (vw), 2970 (w), 2915 (w), 2831 (w), 2770 (vs), 2319 (vw), 2277 (w), 1440 (m), 1410 (s), 1175(m). $C_{12}H_{36}In_3La$ (663.78 g/mol): calculated C 21.71, H 5.47; found C 23.46, H 5.69. Although the values are way outside the range viewed as establishing analytical purity (C: +1.75 %, H: +0.22 %), they are provided to illustrate the best values obtained to date. ICP: La/In/Al = 1:2.7:0.3 (La 8.51 wt.%; In 18.99 wt.%; Al 0.54 wt.%)

Route b): A solution of La(AlMe$_4$)$_3$ (249 mg, 0.621 mmol, 1 equiv.) in *n*-hexane (6 mL) was cooled to –67 °C and THF (0.15 mL, 1.86 mmol 3 equiv.) was added at –67 °C. Instant formation of a colourless precipitate was observed. The precipitate was centrifugated and washed with *n*-hexane (3 mL). Afterwards InMe$_3$ (318 mg, 1.99 mmol, 3.2 equiv.) was added in *n*-hexane (3 mL) at –67 °C. Slowly heating the suspension to 0 °C resulted in a colourless solution. The solution was concentrated *in vacuo* and stored at –40 °C. Crystallization afforded 272 mg (0.409 mmol; 66 %) colourless crystals of La(InMe$_4$)$_3$.

$La_4In_7(C)(CH)_2(CH_2)_2(CH_3)_{19}$ (4a) and $La_5In_9(CH)_6(CH_3)_{24}$ (4b)

Route c): In a pressure tube, La(InMe$_4$)$_3$ (147 mg, 0.222 mmol, 1 equiv.) was dissolved in toluene (8 mL) and heated to 80 °C for 1 hour. An insoluble solid precipitated from a yellow solution. The yellow solution was filtered and stored at –40 °C. Crystallization afforded 16.9 mg colourless and yellow crystals. The colourless crystals were determined to be [$La_4In_7(C)(CH)(CH_2)_2(CH_3)_{19}$] (**4a**). In later investigations (Route d)) it was determined that the yellow crystals were [$La_5In_9(CH)_6(CH_3)_{24}$] (**4b**). ^{1}H NMR (500.1 MHz, thf-d_8, 26 °C): δ = 2.31, 1.88, 1.29, 0.87, -0.39, -0.64, -0.96 ppm.

Route d): A solution of La(AlMe$_4$)$_3$ (186 mg, 0.465 mmol, 1 equiv.) in *n*-hexane (8 mL) was stirred at 0 °C for 30 minutes. Subsequently InMe$_3$ (230 mg, 1.44 mmol, 3.1 equiv.) was added at 0 °C. The reaction mixture was stirred for an additional 15 minutes. Afterwards THF (0.25 mL, 3.1 mmol, 6 equiv.) was added to the reaction mixture, a colourless precipitate formed instantly, which rapidly turned yellow. After washing with *n*-hexane, the precipitate was dried to afford 149 mg of a yellow powder. A fraction of it was dissolved in toluene and stored at –40 °C. After one week several yellow crystals of [$La_5In_9(CH)_6(CH_3)_{24}$] (**4b**) were obtained. DRIFT (KBr, cm^{-1}): 2984 (m), 2909 (vs), 2811 (s), 2283 (vw), 1485 (vw), 1461 (m), 1450 (m), 1369 (vw), 1346 (vw), 1252 (vw), 1182 (s), 1018 (s), 919 (vw), 866 (m), 706 (w), 604 (vw). ^{1}H NMR (500.1 MHz, toluene-d_8, 26 °C): δ = 2.66, 0.90, 0.48, 0.45, 0.44, 0.24-0.19, 0.08-0.06, -0.05, -0.33 ppm. $C_{30}H_{78}In_9La_5$ (3902.05 g/mol): calculated C 16.63, H 3.63; found C 28.36, H 5.94. Although the values are way outside the range viewed as establishing analytical purity (C: +11.73 %, H: +2.31 %), they are provided to illustrate the best values obtained to date. ICP: In/Al = 5.7:1.

$[(Me_3TACN)_2LaMe_2][InMe_4]$ (5)

La(InMe$_4$)$_3$ (342 mg, 0.515 mmol, 1 equiv.) was dissolved in *n*-hexane (8 mL) and stirred at –67 °C. Afterwards an excess of THF (2 mL) was added. Instant precipitation of a colourless solid occurred. The solid was centrifugated and washed with cold *n*-hexane at –67 °C. Subsequently, pre-cooled *n*-hexane (3 mL) and Me$_3$TACN (176 mg, 1.03 mmol, 2 equiv.) were added to the solid. The

reaction mixture was vigorously shaken and allowed to slowly warm to 0 °C after which the mixture was filtered and stored at –40 °C. Crystallization afforded 43.4 mg (0.09 mmol, 17 %) of compound **5**. DRIFT (KBr, cm^{-1}): 3911 (vw), 3775 (vw), 3663 (vw), 2998 (vw), 2927 (vw), 2810 (w), 2386 (w), 2349 (vw), 2300 (vw), 2191 (vw), 1765 (vw), 1600 (vw), 1494 (vs), 1488 (vs), 1462 (vs), 1451 (s), 1371 (w), 1308 (m), 1268 (vw), 1206 (vw), 1148 (vw), 1079 (w), 1010 (s), 884 (w), 760 (m), 692 (vw), 648 (w), 574 (vw), 542 (vw), 434 (w). ^{1}H NMR (500.1 MHz, toluene-d_8, 0 °C): δ = 2.61 (s, NCH_2, 15H), 2.23 (s, NCH_3, 18H), 2.18 (s, NCH_2, 9H), 1.58 (m, CH_3, 6H), 0.06 (br, InCH_3 and La CH_3, 18H) ppm. ^{13}C NMR (125.8 MHz, toluene-d_8, 0 °C): δ = 57.79 (NCH$_2$), 55.58 (CH$_3$), 47.46 (NCH$_3$), 47.24 (NCH$_2$) ppm. $C_{24}H_{60}InLaN_6$ (686.51 g/mol): calculated C 41.99, H 8.81, N 12.24; found C 43.66, H 8.74, N 11.74. (C: +1.67 %, H: -0.07 %, N: -0.5 %).

Ce(InMe$_4$)$_3$ (6)

A solution of Ce(AlMe$_4$)$_3$ (265 mg, 0.661 mmol, 1 equiv.) in *n*-hexane (8 mL) was cooled to 0 °C. Subsequently, InMe$_3$ (359 mg, 2.25 mmol, 3.4 equiv.) dissolved in *n*-hexane (2 mL) and THF (0.08 mL, 0.99 mmol, 1.5 equiv.) was added at 0 °C. After vigorous stirring for 20 minutes, THF (0.09 mL, 1.2 mmol, 1.7 equiv.) was added to the solution over 1 hour. Following additional stirring for 40 minutes, toluene (2 mL) was added, and the resulting solution was concentrated *in vacuo* and stored at –40 °C. Crystallization afforded 315 mg (0.474 mmol, 72%) yellow crystals of Ce(InMe$_4$)$_3$ (**6**). DRIFT (KBr, cm^{-1}): 3938 (w), 3775 (w), 3663 (m), 2979 (vw), 2915 (vw), 2831 (vw), 2772 (w), 2388 (s), 2349 (m), 2278 (vs), 1765 (w), 1726 (w), 1631 (m), 1479 (s), 1462 (s), 1443 (vs), 1177 (m), 1148 (m), 1016 (vw), 865 (vw), 717 (w), 543 (vw), 498 (w), 404 (vw). ^{1}H NMR (500.1 MHz, toluene-d_8, 0 °C): δ = 2.43 (br, s, 36H, CH_3) ppm. $C_{13.50}H_{40.50}Al_{1.50}CeIn_{2.01}$ (613.63g/mol): calculated C 26.39, H 6.65; found C 22.83, H 5.48. Although the C and H values are outside the range viewed as establishing analytical purity (C: -3.56 %, H: -1.17 %), they are provided to illustrate the best values obtained to date. ICP: In/Al = 6.7:1.

Nd(InMe$_4$)$_3$ (7)

A solution of Nd(AlMe$_4$)$_3$ (214 mg, 0.527 mmol, 1 equiv.) in *n*-hexane (8 mL) was cooled to 0 °C. Subsequently, InMe$_3$ (286 mg, 1.79 mmol, 3.4 equiv.) dissolved in *n*-hexane (2 mL) and THF (0.06 mL, 0.79 mmol,1.5 equiv.) was added at 0 °C. After vigorous stirring for 20 minutes, THF (0.07 mL; 0.90 mmol; 1.7 equiv.) was added to the solution over 1 hour. Following additional stirring for 40 minutes, toluene (2 mL) was added, and the resulting solution was concentrated *in vacuo* and stored at –40 °C. Recrystallization afforded 190 mg (0.285 mmol; 54%) blue crystals of Nd(InMe$_4$)$_3$ (**7**). DRIFT (KBr, cm^{-1}): 3086 (vw), 3017 (w), 2979 (w), 2916 (w), 2809 (w), 2775 (m), 2295 (w), 2274 (w), 1443 (m), 1410 (m), 1178 (s), 1147 (vs), 1111 (vw), 1039 (vw), 1015 (w), 920 (vw), 868 (w), 724 (m), 585 (vw), 548 (vw), 500 (vw), 476 (vw), 459 (vw). $C_{12}H_{36}NdIn_3$ (669.11 g/mol): calculated C 21.54, H 5.42; found C 24.14, H 5.77. Although the C value is outside the range viewed as establishing analytical purity (C: +2.6 %, H: +0.35 %), they are provided to illustrate the best values obtained to date. ICP: In/Al = 3.8:1.

$Ce_3(In/Al)_4(CH)(CH_3)_{18}$(thf) (8)

A solution of $Ce(AlMe_4)_3$ (77.1 mg, 0.192 mmol, 1 equiv.) in *n*-hexane (4 mL) was cooled to 0 °C. Subsequently, $InMe_3$ (92.2 mg, 0.577 mmol, 3 equiv.) dissolved in *n*-hexane (2 mL) and THF (0.05 mL, 0.67 mmol, 3.5 equiv.) was added at 0 °C. After vigorous stirring for 10 minutes a yellow suspension was formed. The suspension was filtered, and the resulting solution was stored at –40 °C. Crystallization afforded 51.3 mg (0.045 mmol; 23 %) yellow crystals of **8**. DRIFT (KBr, cm^{-1}): 3910 (w), 3791 (w), 3663(w), 2960 (w), 2910 (w), 2806 (w), 2775 (m), 2386 (vs), 2349 (w), 2301 (m), 1765 (vw), 1726 (w), 1600 (m), 1494 (s), 1462 (vs), 1451 (vs), 1190 (s), 1010 (vs), 856 (s), 700 (s), 585 (vw), 495 (w), 410 (w). $C_{26.5}H_{67}Al_{0.39}Ce_3In_{3.61}O$ (1246.74 g/mol): calculated C 25.52, H 5.42; found C 26.85, H 5.77. Although the C value is outside the range viewed as establishing analytical purity (C: +1.33 %, H: +0.35 %), they are provided to illustrate the best values obtained to date. ICP: In/Al = 1:1.5.

NMR Spectra

In general, solvent signals are labeled with an asterisk (*). In some cases, the paramagnetic nature of Ce(III) and Nd (III) did not allow for conclusive NMR analysis.

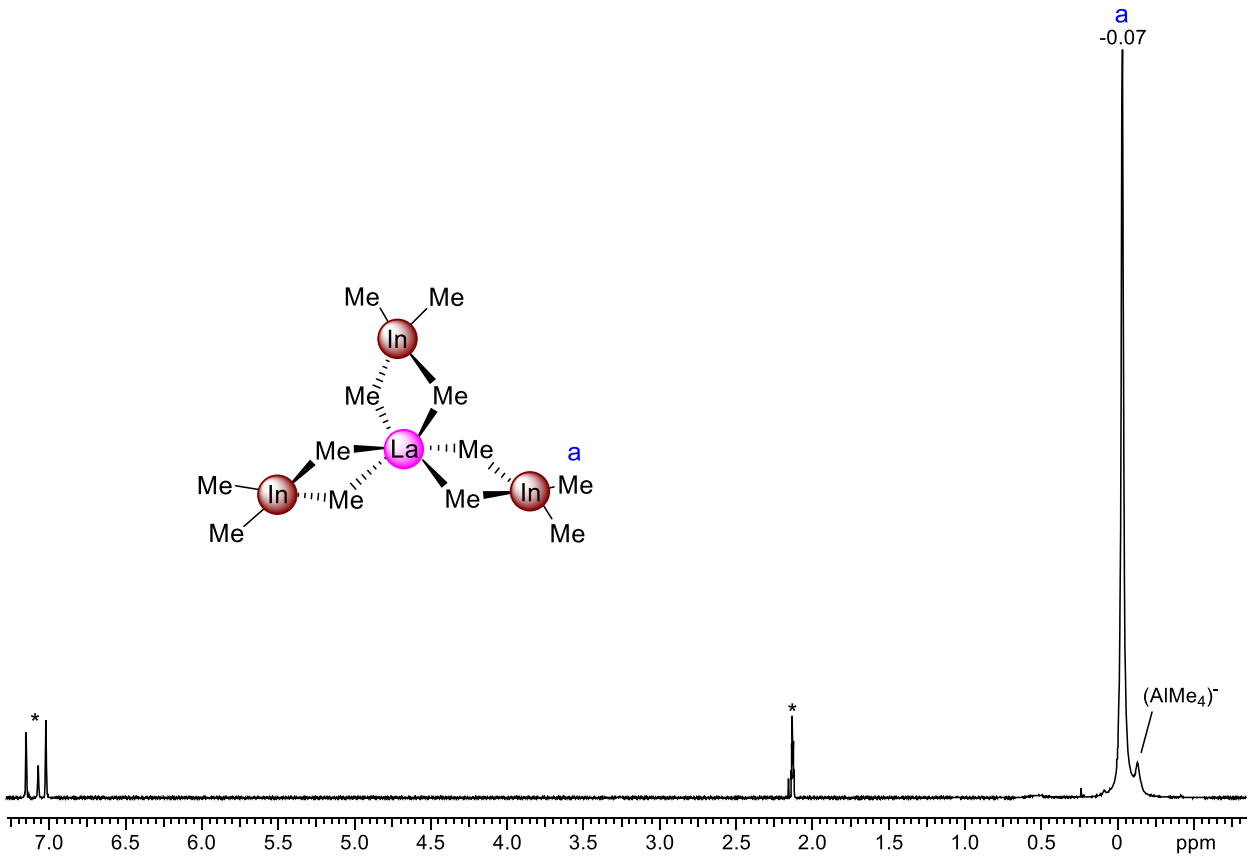

Figure S1. ^{1}H NMR spectrum (500 MHz, toluene-d_8, 0 °C) of La(InMe$_4$)$_3$ (**3**).

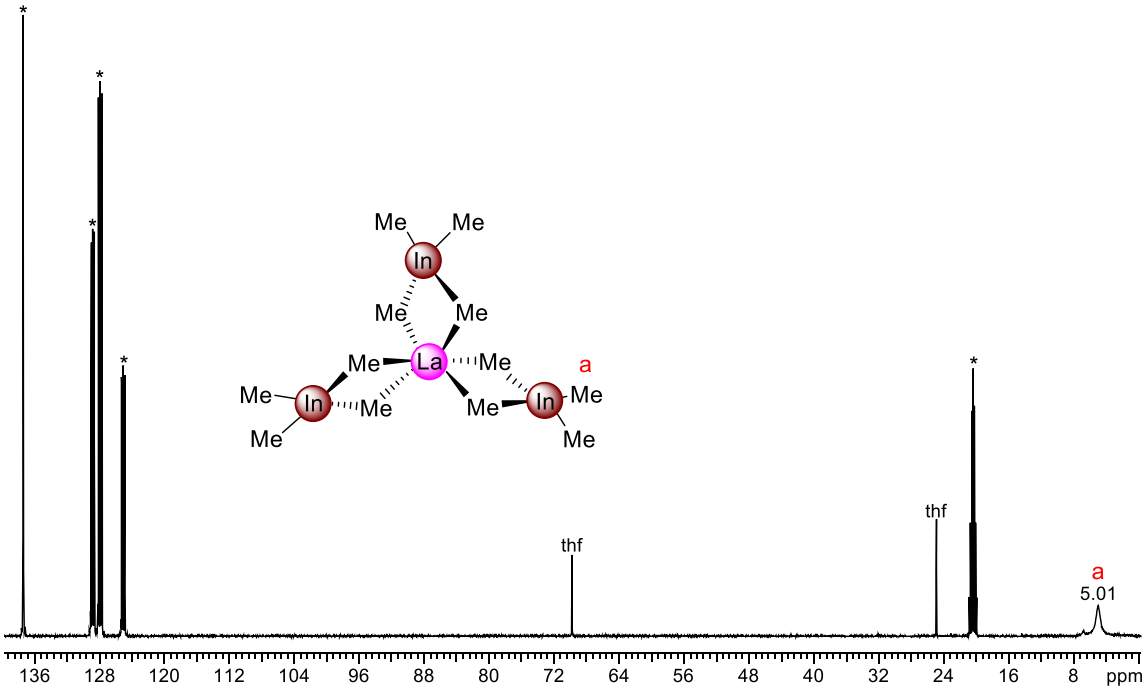

Figure S2. ^{13}C NMR spectrum (126 MHz, toluene-d_8, 0 °C) of La(InMe$_4$)$_3$ (**3**).

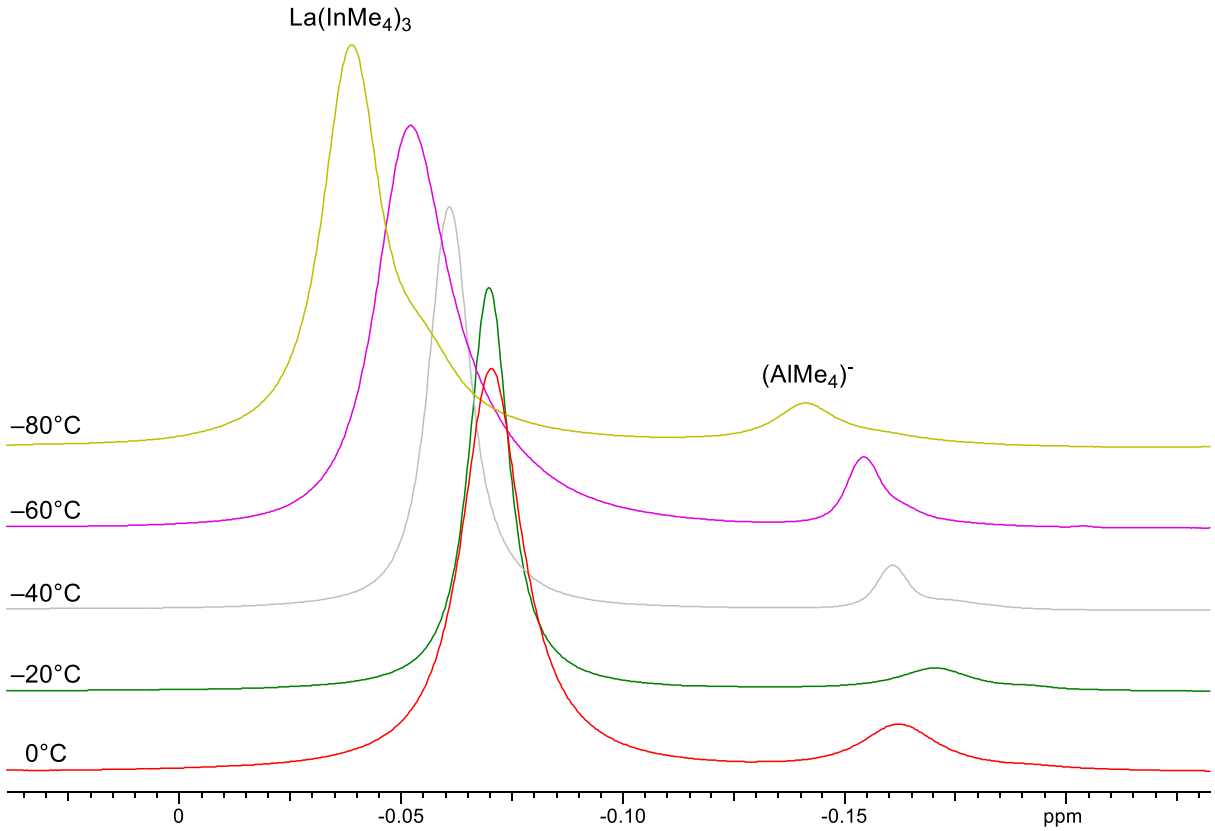

Figure S3. VT ^{1}H NMR spectra (500 MHz, toluene-d_8, 0 °C to –80 °C) of La(InMe$_4$)$_3$ (**3**).

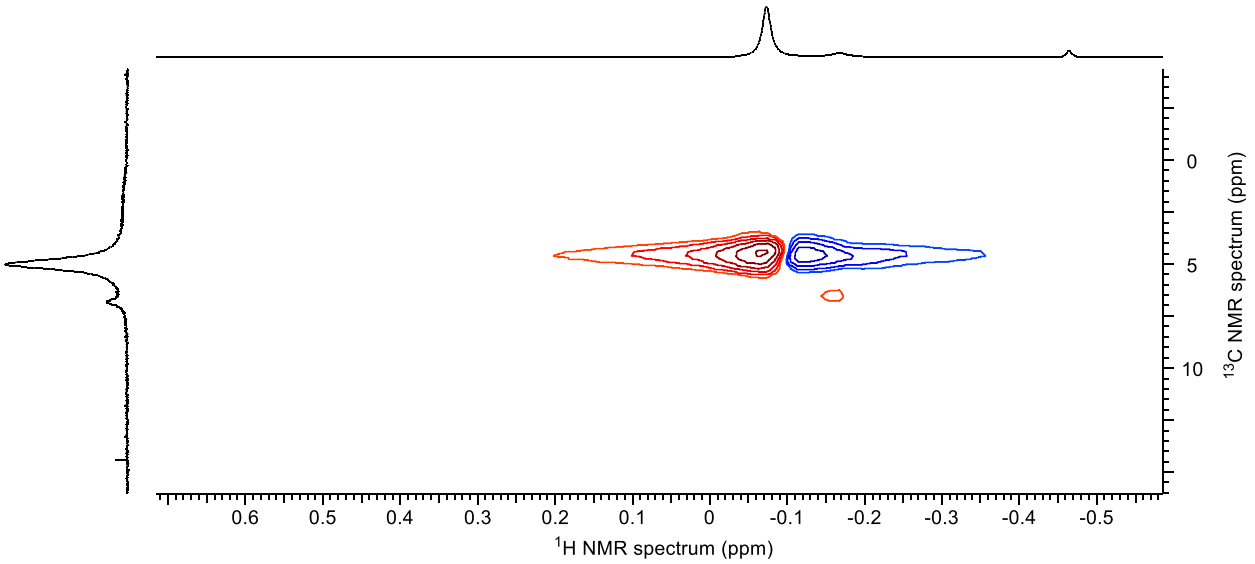

Figure S4. ^{1}H-^{13}C HSQC NMR spectrum (500/126 MHz, toluene-d_8, 0 °C) of La(InMe$_4$)$_3$ (**3**).

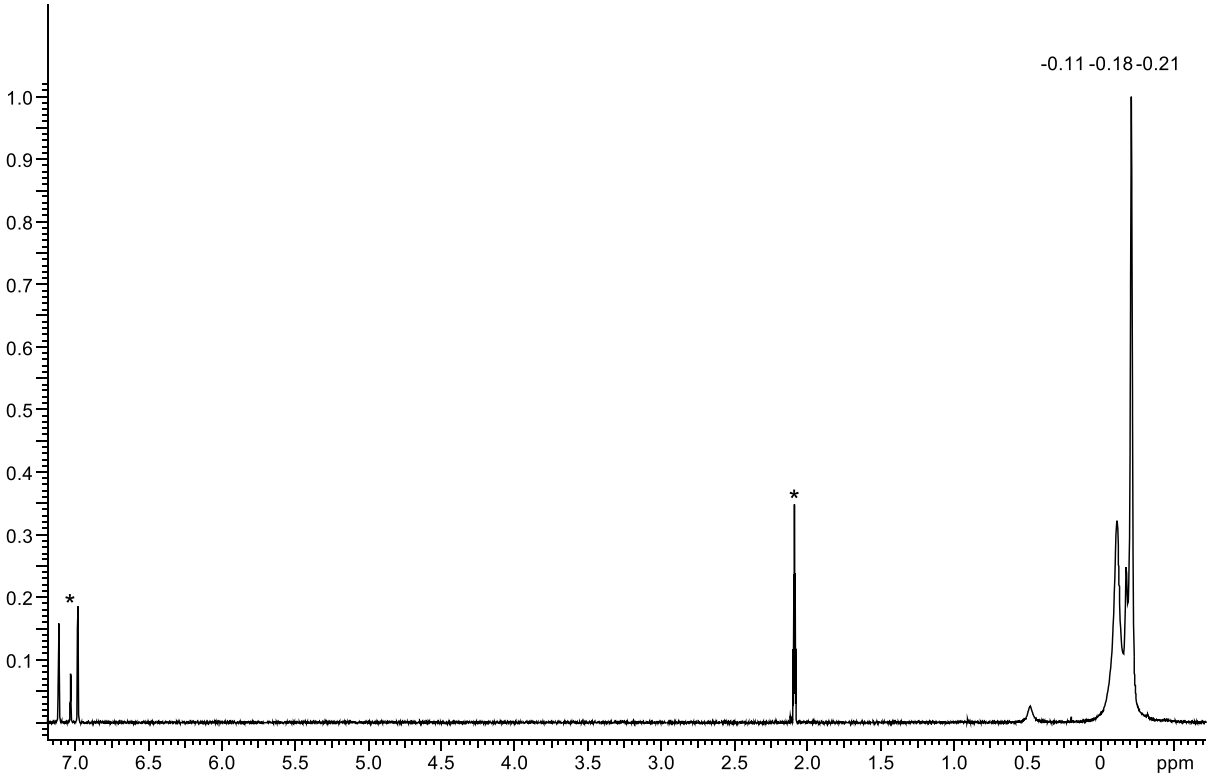

Figure S5. ^{1}H NMR spectrum (500 MHz, toluene-d_8, 0 °C) of La(InMe$_4$)$_3$: La(AlMe$_4$)$_3$ (1:1).

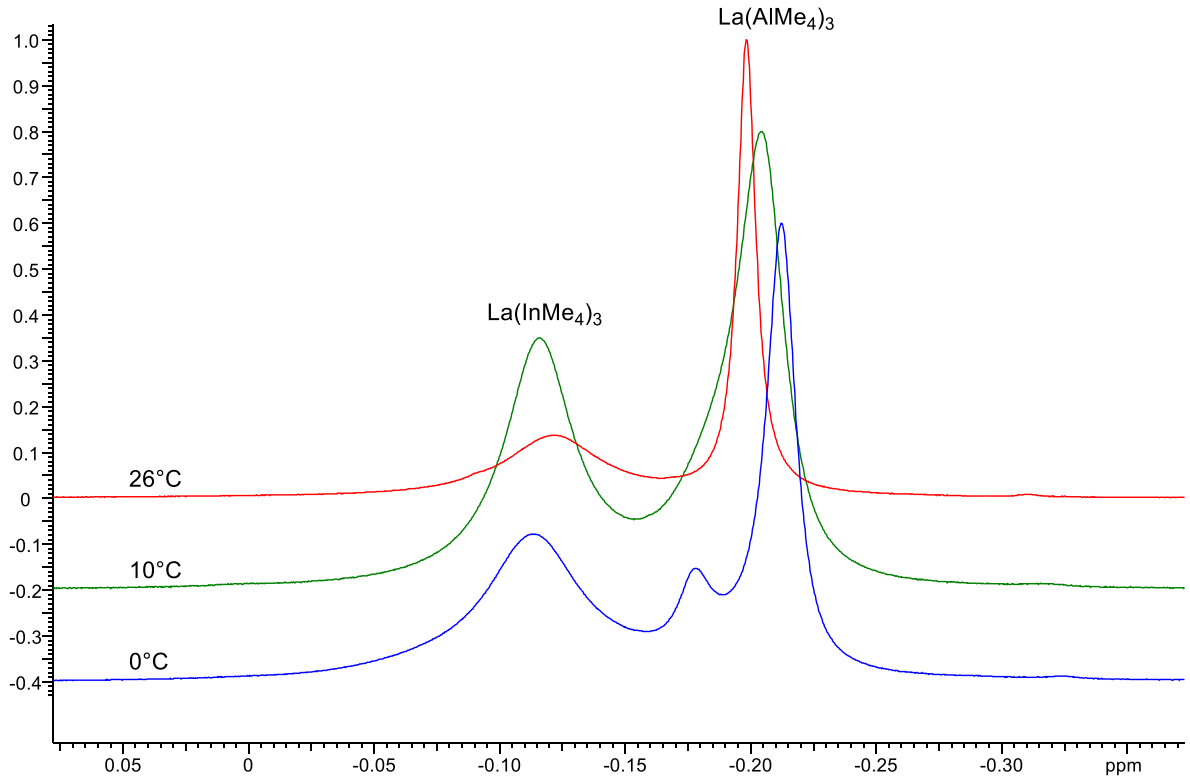

Figure S6. VT ^{1}H NMR spectra (500 MHz, toluene-d_8, 0 °C to 26 °C) of $La(InMe_4)_3$: $La(AlMe_4)_3$(1:1).

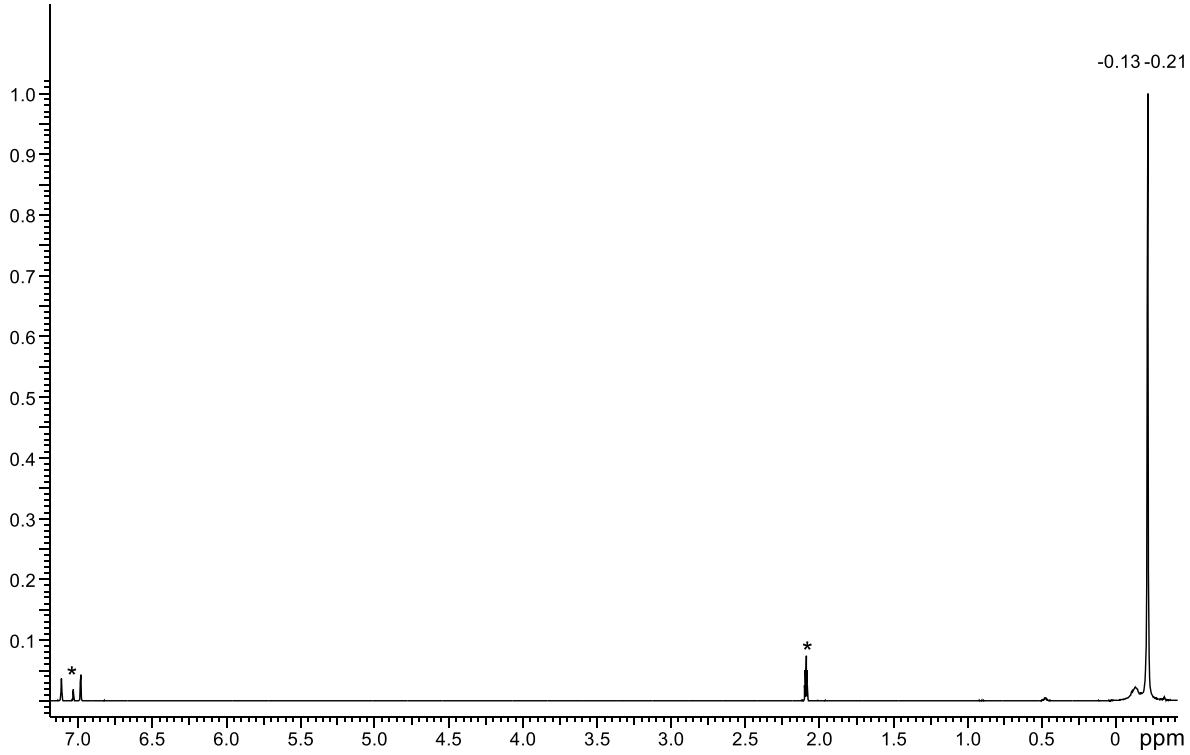

Figure S7. ^{1}H NMR spectrum (500 MHz, toluene-d_8, 0 °C) of $La(InMe_4)_3$: $La(AlMe_4)_3$ (1:10).

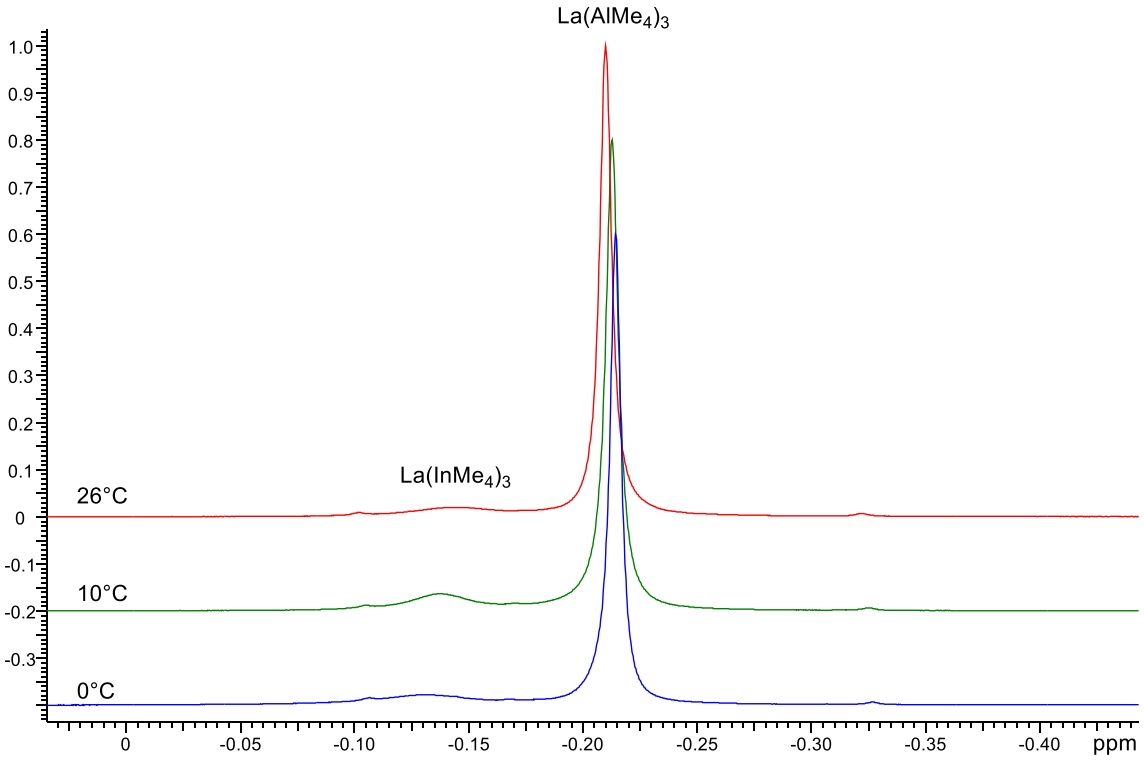

Figure S8. VT ^{1}H NMR spectra (500 MHz, toluene-d_8, 0 °C to 26 °C) of $La(InMe_4)_3$: $La(AlMe_4)_3$ (1:10).

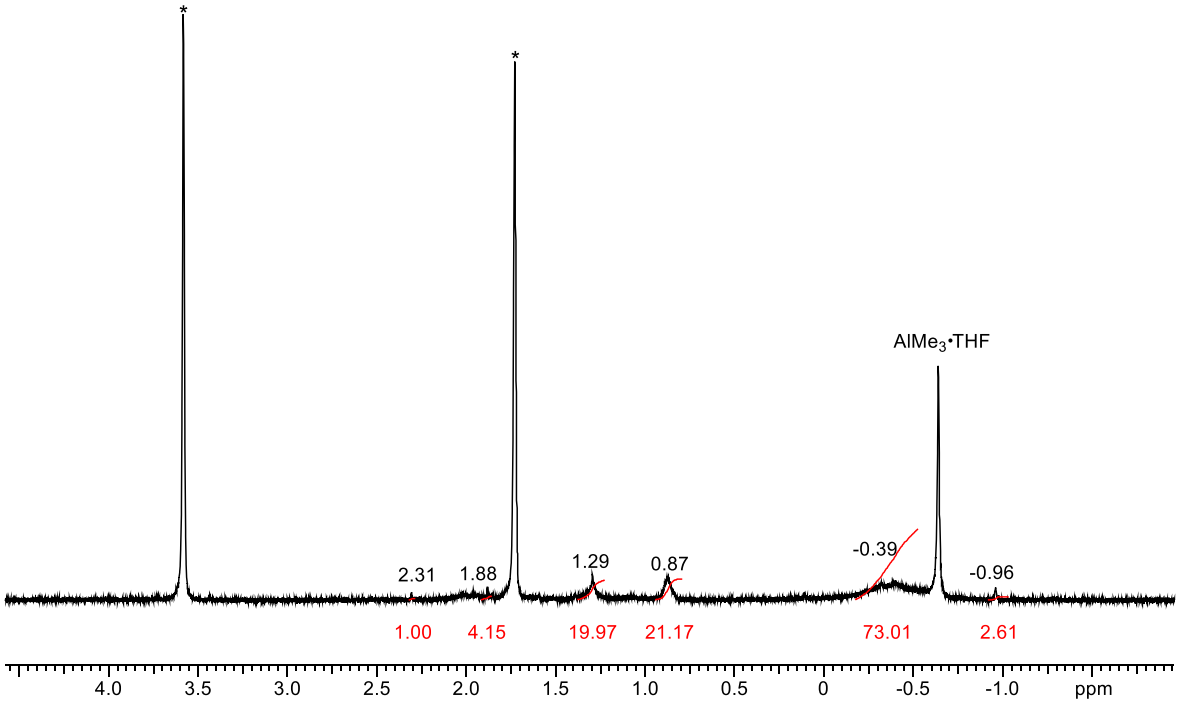

Figure S9. ^{1}H NMR spectrum (500 MHz, THF-d_8, 26 °C) of $[La_4In_7(C)(CH)_2(CH_2)_2(CH_3)_{19}]$ (**4a**) and $[La_5In_9(CH)_6(CH_3)_{24}]$ (**4b**) (Route c).

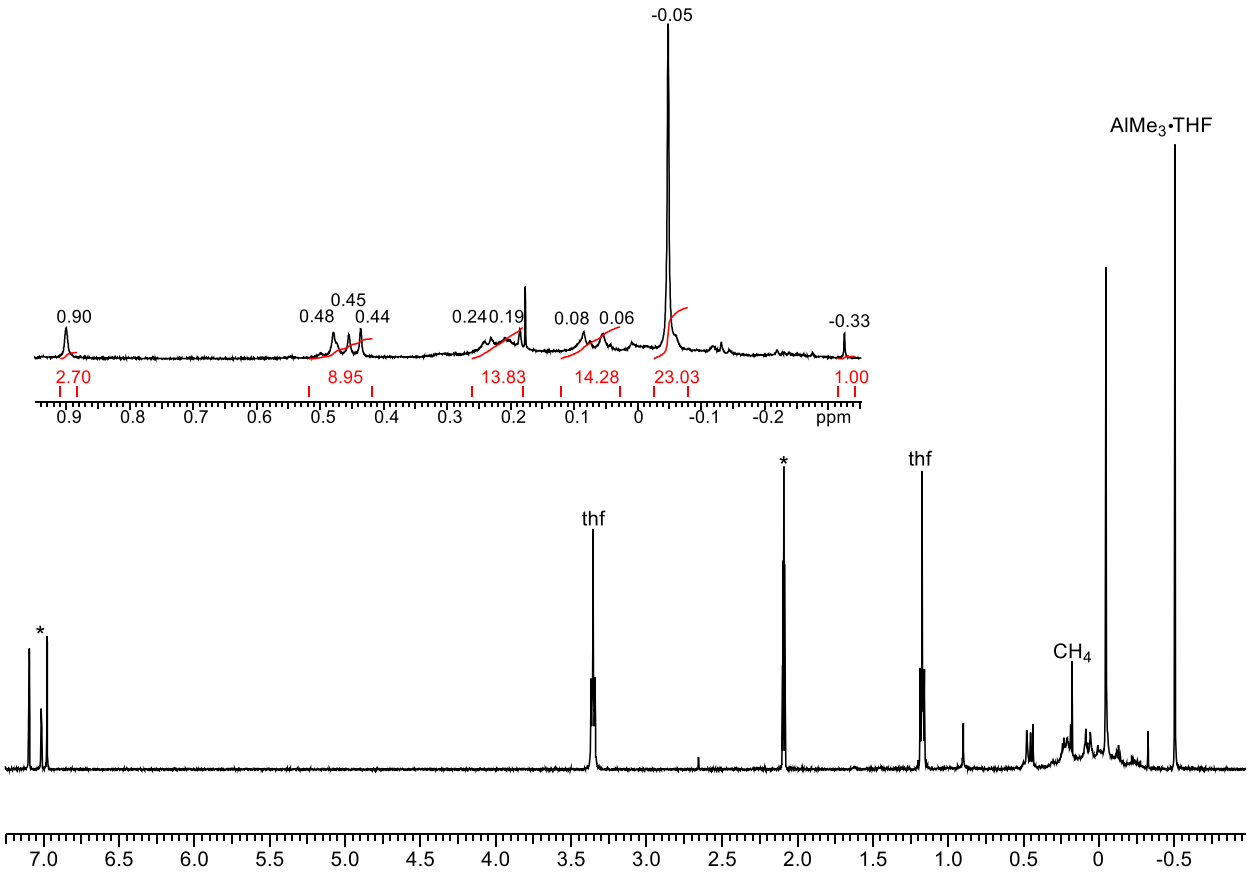

Figure S10. ^{1}H NMR spectrum (500 MHz, toluene-d_8, 26 °C) of $[La_4In_7(C)(CH)_2(CH_2)_2(CH_3)_{19}]$ (**4a**) and $[La_5In_9(CH)_6(CH_3)_{24}]$ (**4b**) (Route d).

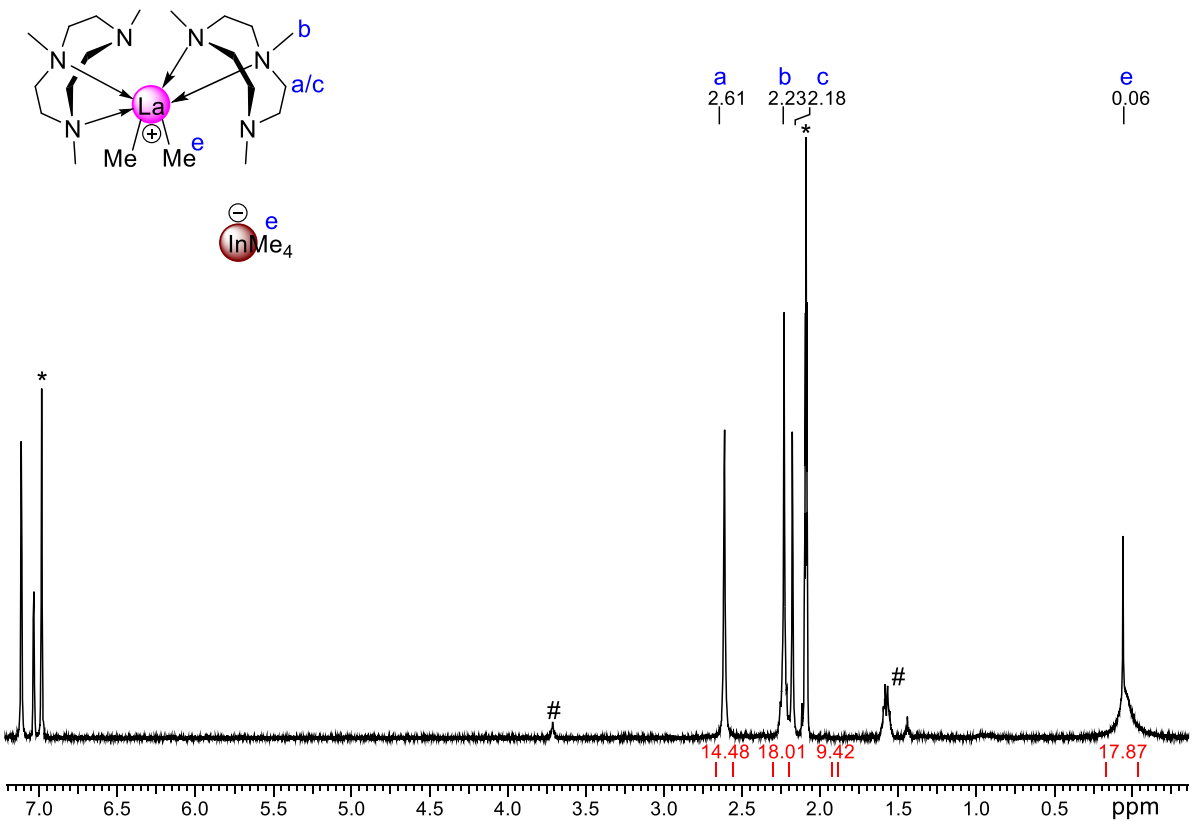

Figure S11. ^{1}H NMR spectrum (500 MHz, toluene-d_8, 0 °C) of [(Me$_3$TACN)$_2$LaMe$_2$][InMe$_4$] (**5**) (# marks unidentified side product and residual THF).

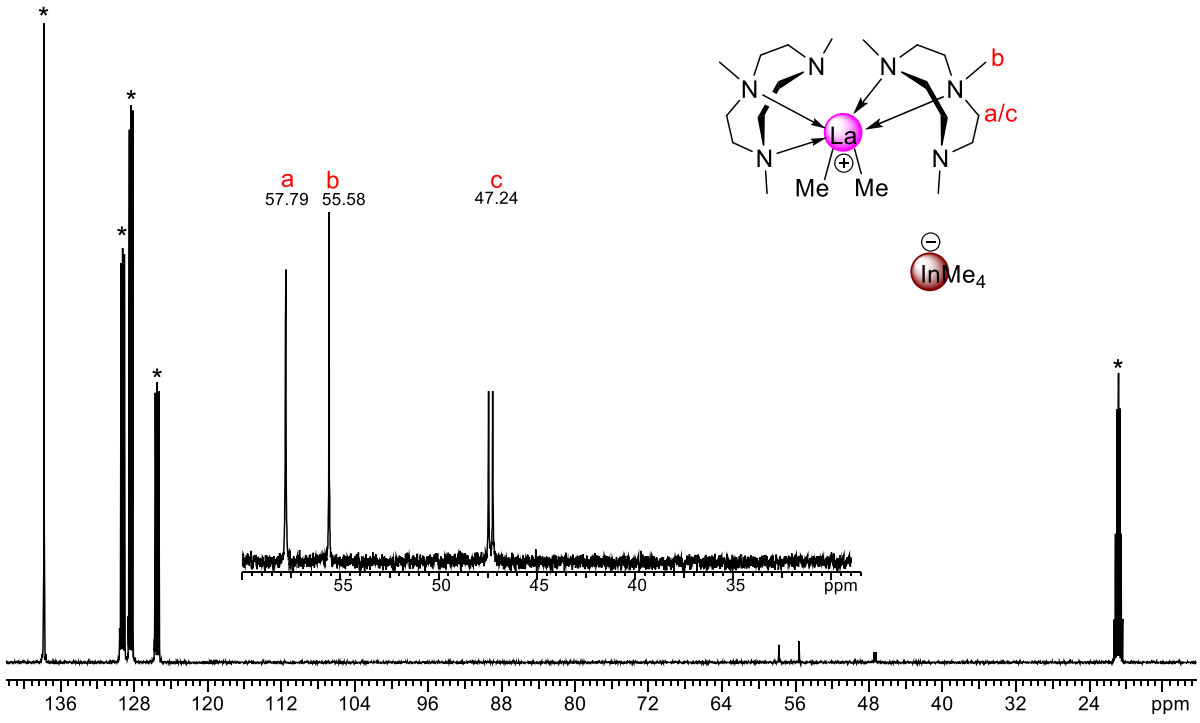

Figure S12. ^{13}C NMR spectrum (126 MHz, toluene-d_8, 0 °C) of [(Me$_3$TACN)$_2$LaMe$_2$][InMe$_4$] (**5**).

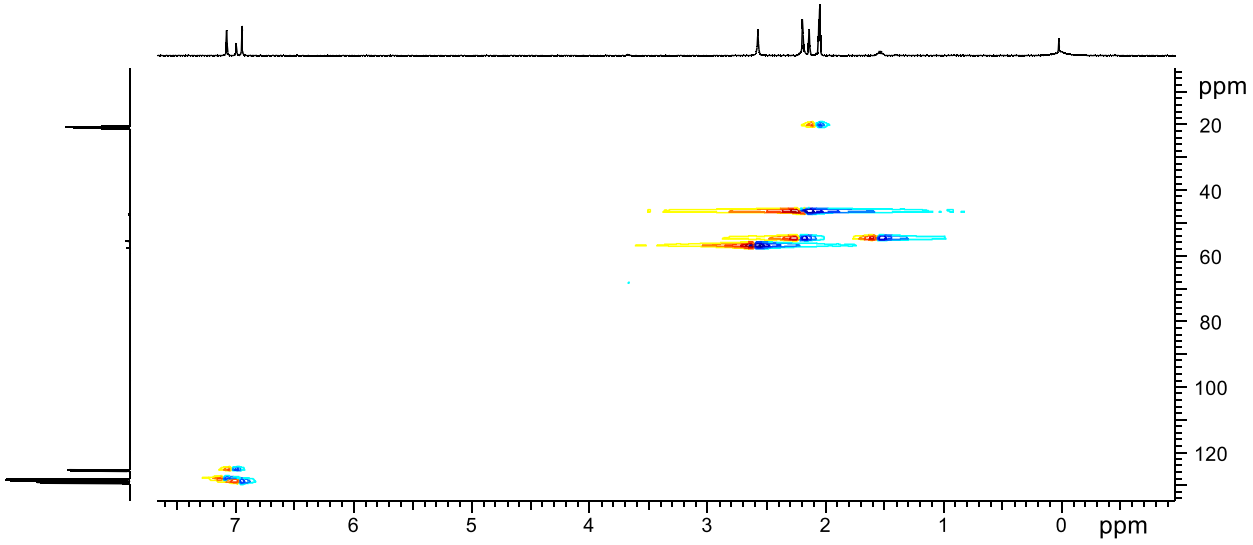

Figure S13. ^{1}H-^{13}C HSQC NMR spectrum (500/126 MHz, toluene-d_8, 0 °C) of $[(Me_3TACN)_2LaMe_2][InMe_4]$ (**5**).

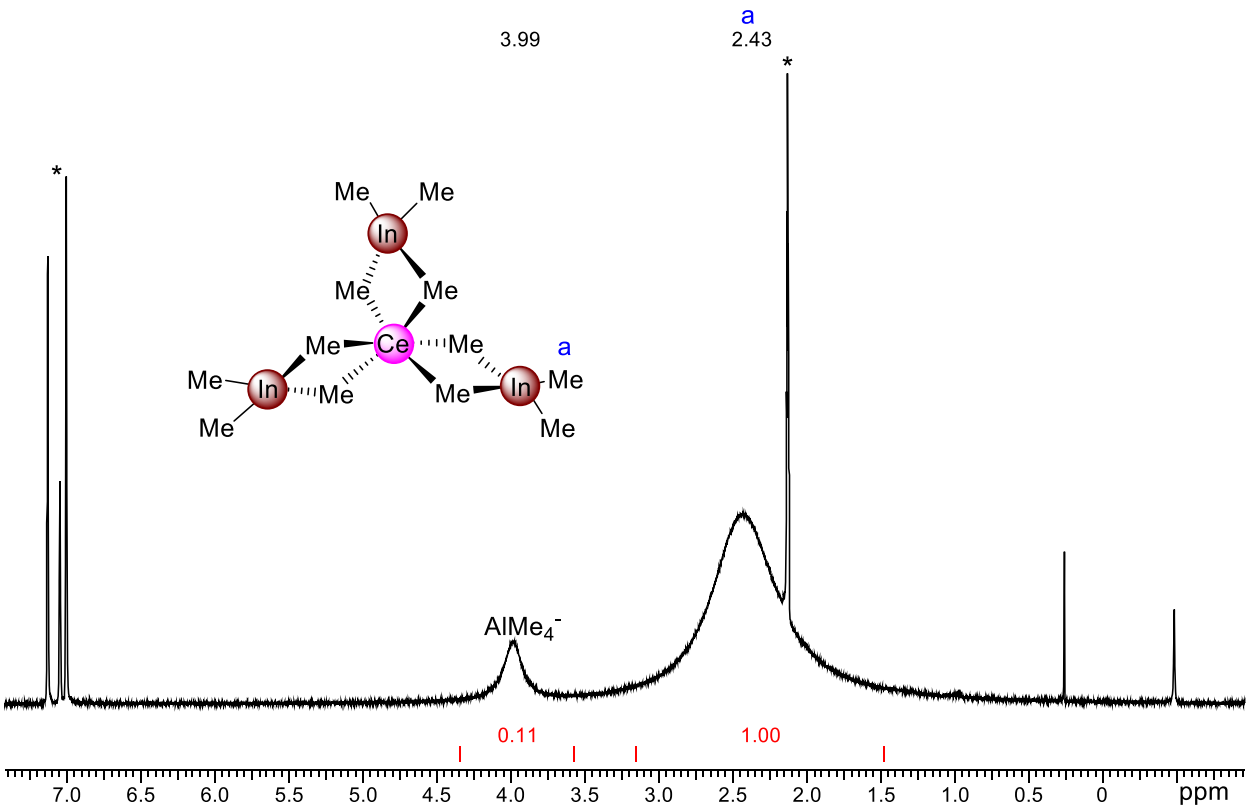

Figure S14. ^{1}H NMR spectrum (500 MHz, toluene-d_8, 0 °C) of $Ce(InMe_4)_3$ (**6**).

IR Spectra

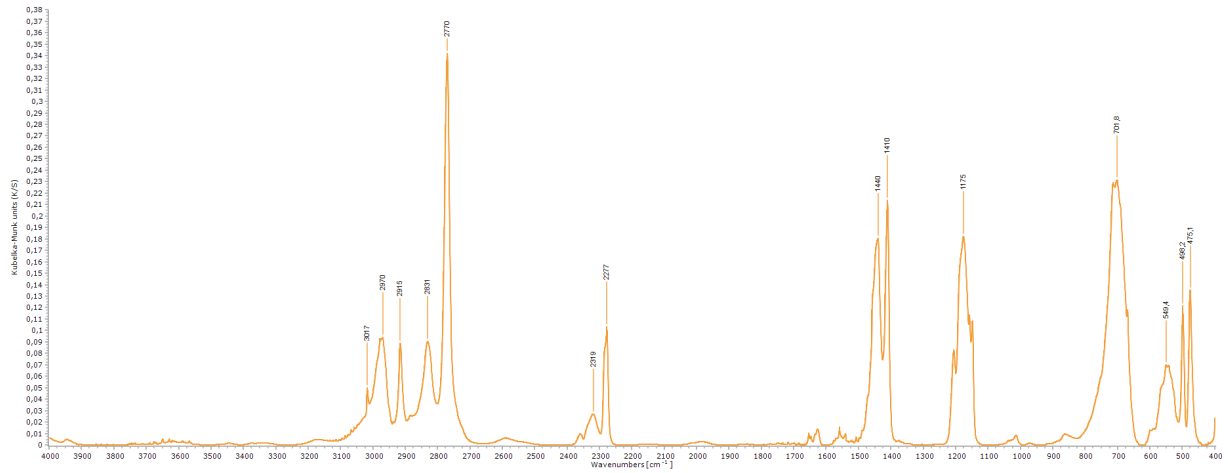

Figure S15. DRIFT spectrum of complex **3**.

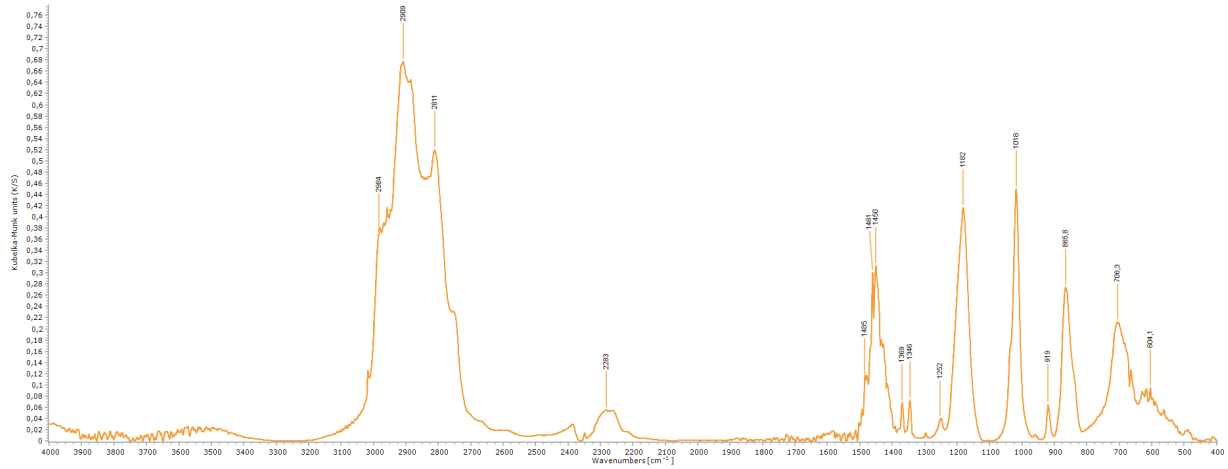

Figure S16. DRIFT spectrum of complex **4**.

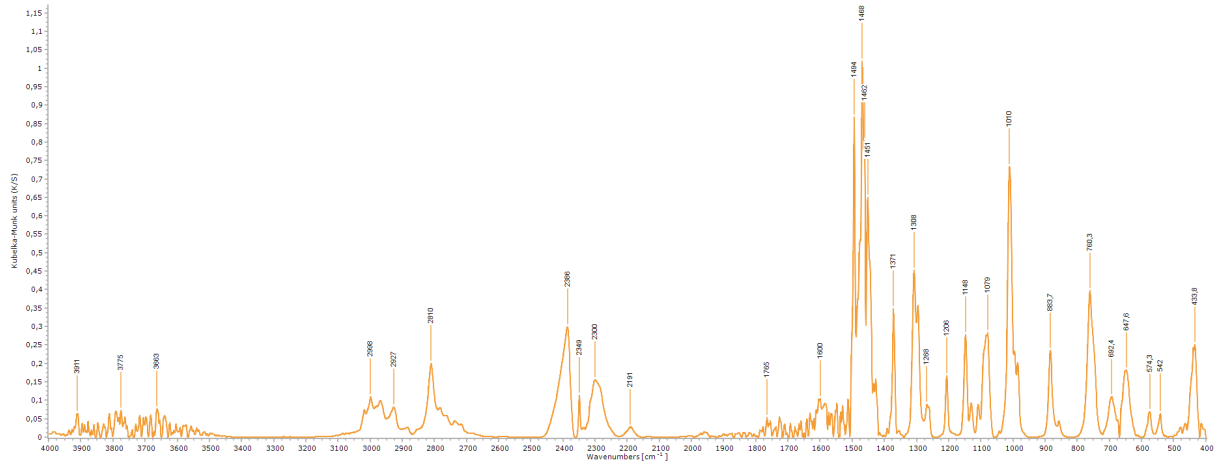

Figure S17. DRIFT spectrum of complex **5**.

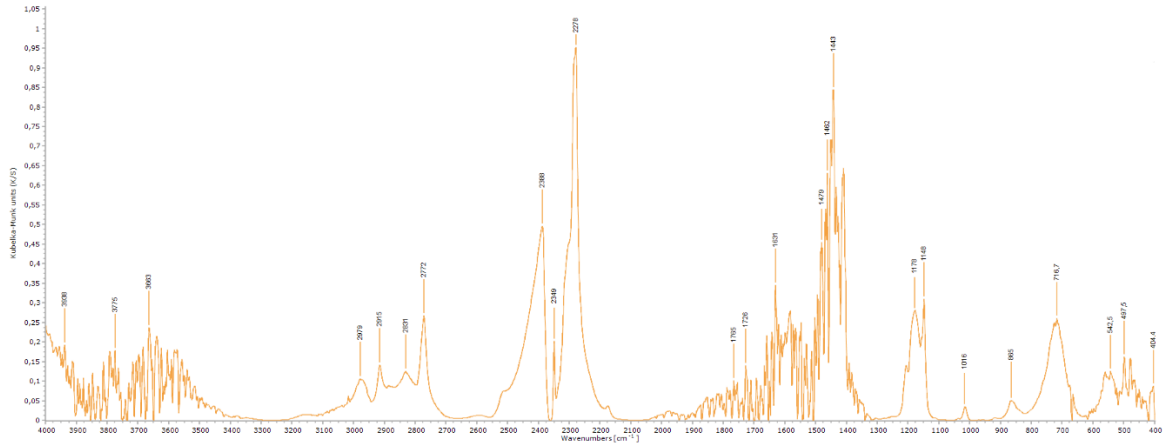

Figure S18. DRIFT spectrum of complex **6**.

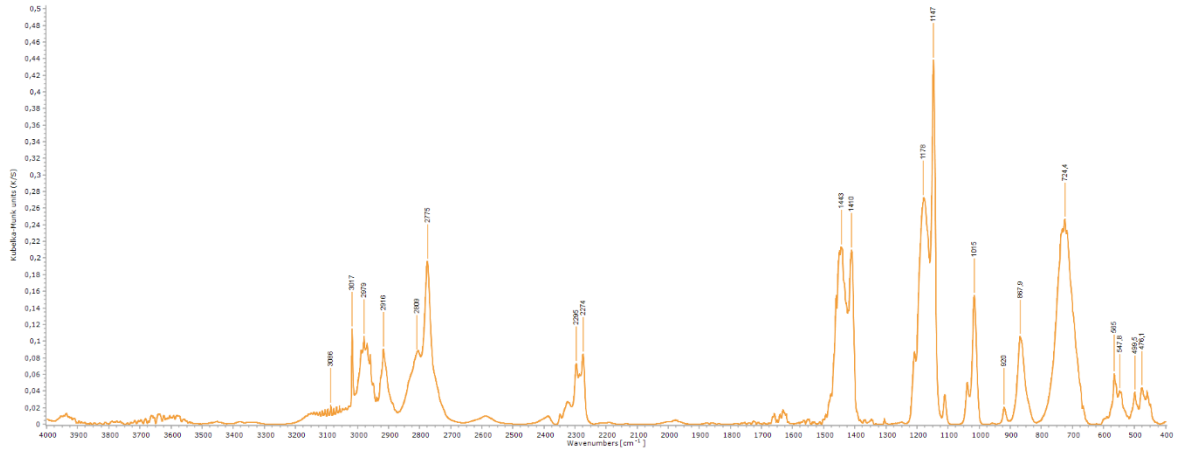

Figure S19. DRIFT spectrum of complex **7**.

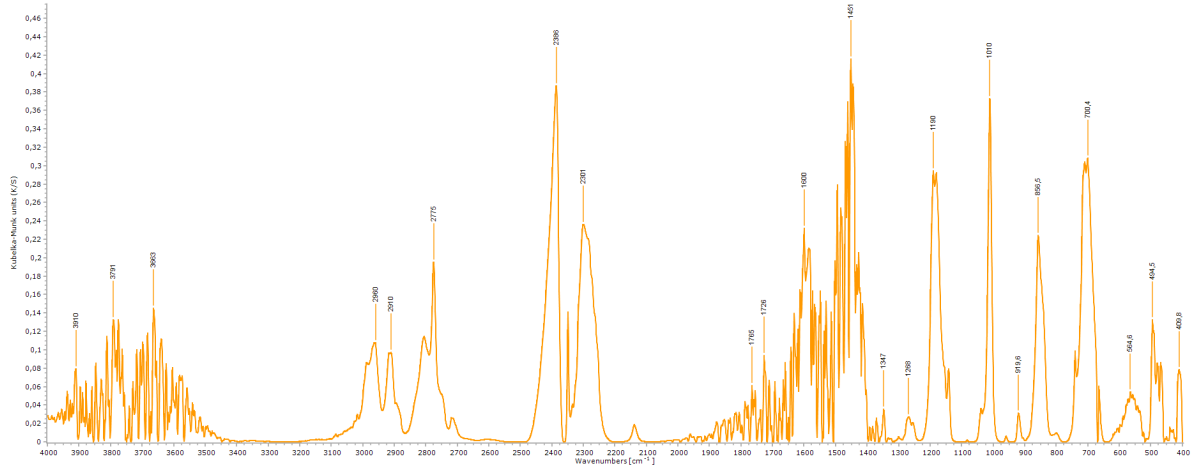

Figure S20. DRIFT spectrum of complex **8**.

Crystallography

Crystal structure determination

Single crystals suitable for X-ray diffraction were selected inside a glovebox and coated with Parabar (10312 Hampton Research) on a glass fiber. X-ray data for all compounds were recorded on a Bruker APEX II DUO diffractometer equipped with an IμS microfocus sealed tube and QUAZAR optics for MoKα (λ = 0.71073 Å). The data collection strategy was determined using COSMO,[2] employing ω-scans. Raw data were processed using APEX,[3] and SAINT.[4] Corrections for absorption effects were applied using SADABS.[5] The structures were solved by direct methods and refined against all data by full-matrix least-squared methods on F^2 using SHELXTL,[6] and ShelXle.[7] In case of **6**, two out of four indium atoms show disorder between In and Al, while for **8** all three indium atoms of the complex show disorder in different ratios. For **8**, disorder of the toluene was calculated using DSR, a program for refining structures in ShelXl[8] and only a connectivity could be shown, which is isostructural to a known aluminium complex. All graphics were produced employing Mercury 2022.2[9] and POV-Ray12.[10]

Single crystals of **3**, **4a**, **4b**, **6** and **7** were grown from saturated toluene solutions at –40 °C. All other crystals were grown from saturated *n*-hexane solutions at –40 °C.

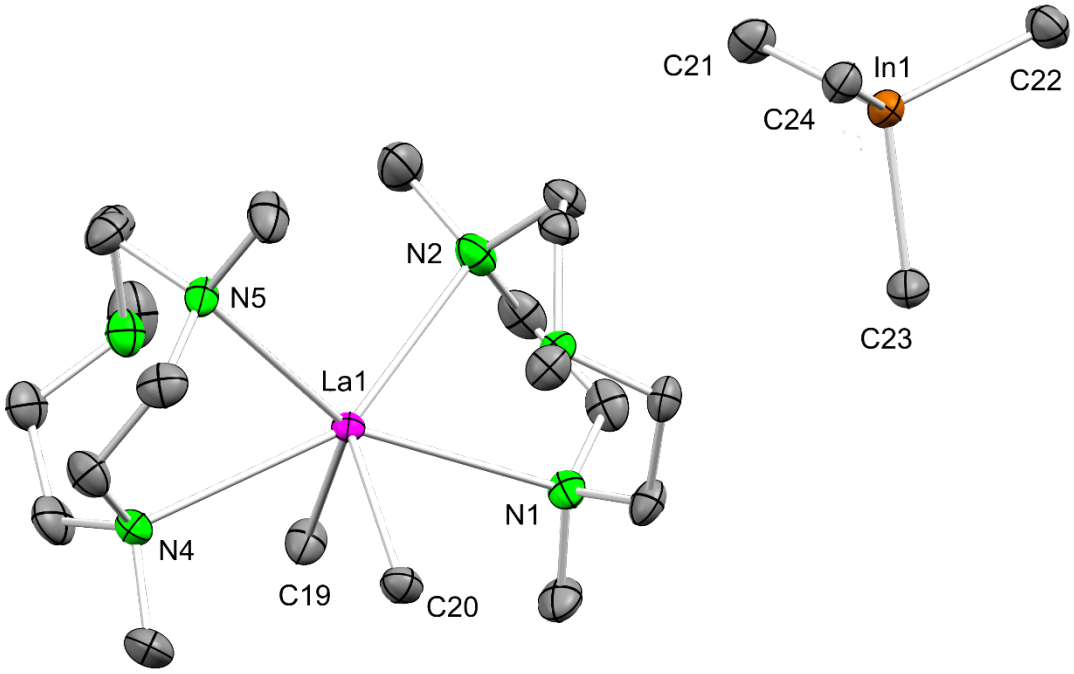

Figure S21. Crystal structure of **5**, with atomic displacement parameters set at 50%. Hydrogen atoms have been omitted for clarity. Selected interatomic distances (Å) and angles (°): La1–C19 2.544(3), La1–C20 2.572(3), La1–N1 2.902(2), La1–N2 2.812(2), La1–N4 2.904(2), La–N5 2.833(2), In1–C21 2.214(3), In1–C22 2.215(3), In1–C23 2.217(3), In1–C24 2.227(3); C19–La1–C20 99.56(9), N1–La1–N2 63.85(7), N4–La1–N5 63.56(6), N1–La1–N5 153.72(6), N1–La1–N4 139.96(6), C21–In1–C22 110.04(11), C21–In1–C24 110.08(10).

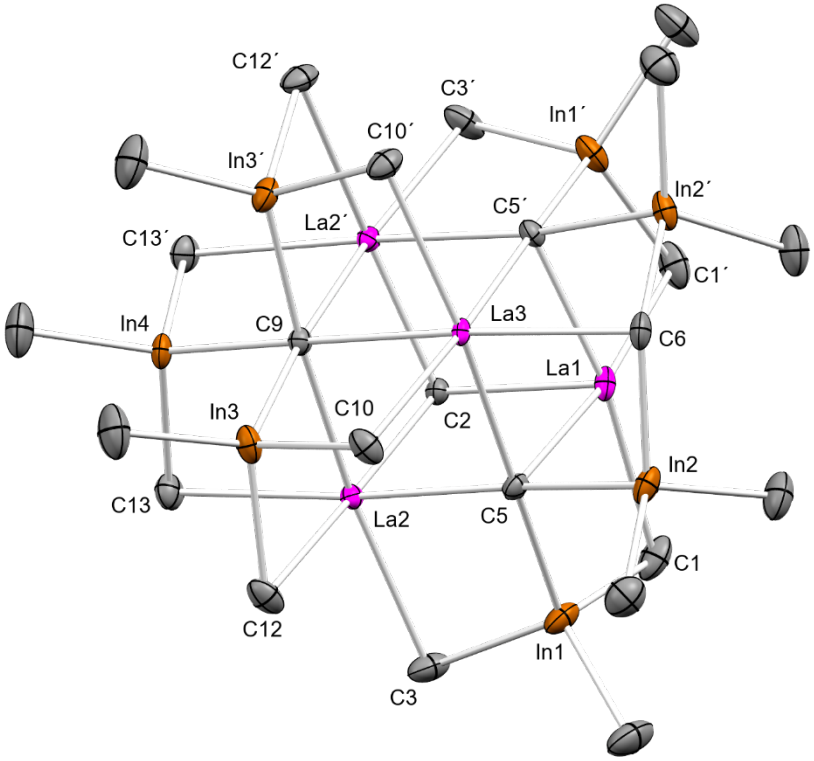

Figure S22. Crystal structure of **4a**, with atomic displacement parameters set at 50%. Hydrogen atoms and co-crystallizing toluene have been omitted for clarity. Selected interatomic distances (Å): La1–C1 2.837(6), La1–C2 2.683(7), La1–C5 2.513(5), La2–C2 2.516(5), La2–C3 2.835(6), La2–C5 2.630(5), La2–C9 2.587(5), La2–C12 2.810(5), La2–C13 2.820(5), La3–C5 2.643(5), La3–C6 2.651(7), La3–C9 2.654(7), La3–C10 2.787(5), In1–C1 2.253(7), In1–C3 2.265(6), In1–C5 2.340(5), In2–C5 2.354(5), In2–C6 2.277(4), In3–C9 2.320(4), In3–C10 2.283(5), In4–C9 2.348(7), In4–C13 2.261(6).

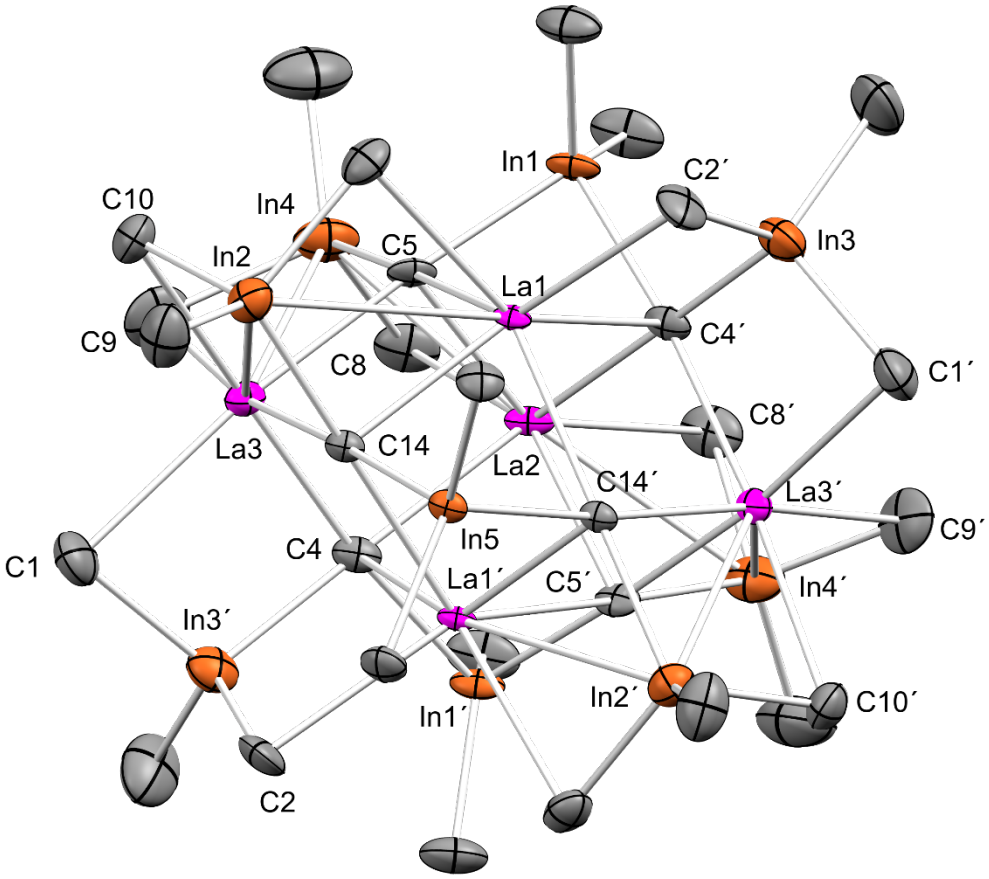

Figure S23. Connectivity of **4b**, with atomic displacement parameters set at 50%. Hydrogen atoms have been omitted for clarity. Selected interatomic distances (Å): La1–C2 2.892(9), La1–C4 2.594(8), La1–C5 2.723(8), La1–C11 2.916(9), La1–C14 2.722(7), La2–C4 2.720(9), La2–C5 2.584(8), La2–C8 2.904(11), La3–C1 2.835(11), La3–C4 2.559(8), La3–C5 2.582(9), La3–C9 2.815(10), La3–C10 2.817(10), La3–C14 2.569(7), In{$InMe_2$}$^+$–C(CH_3) 2.183(10)–2.196(10), In{$InMe_2$}$^+$–C(CH) 2.349(9)–2.365(9), In($InMe_3$)–C(bridging CH_3) 2.211(12)–2.273(13), In($InMe_3$)–C(terminal CH_3) 2.101(16)–2.129(13).

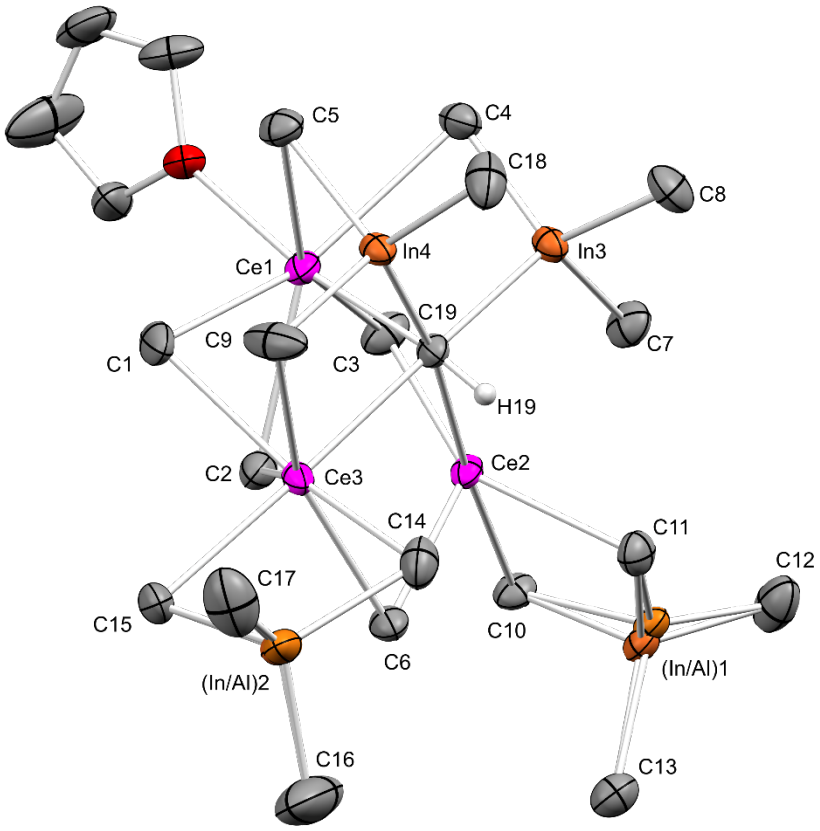

Figure S24. Crystal structure of **8**, with atomic displacement parameters set at 50%. Hydrogen atoms except H19 and co-crystallizing toluene have been omitted for clarity. Selected interatomic distances (Å) and angles (°): Ce1–C(CH_3) 2.636(5)–2.932(5),Ce1–C19 2.477(4), Ce1---In3 3.3359(4), Ce1---In4 3.3105(4), Ce2–C(CH_3) 2.678(5)–2.779(5), Ce2–C19 2.615(4), Ce2---In3 3.3359(4), Ce2---In4 3.3105(4), Ce3–C(CH_3) 2.680(4)–2.937(6), Ce3–C19 2.596(4), Ce3---In2 3.3688(12), Ce3---In4 3.3735(4), In3–C19 2.329(4), In4–C19 2.343(4), In1–C(CH_3) 2.128(5)–2.248(5), In2–C(CH_3) 2.122(7)–2.237(5), Ce1---Ce2 3.5449(3), Ce1---Ce3 3.5470(4), Ce2---Ce3 3.5992(3) ; Ce2–C6–Ce3 84.40(13), Ce3–C19–In3 172.80(19), Ce3–C19–Ce2 87.38(12), Ce3–C19–Ce1 88.71(13), In1–C10–Ce2 83.56(13), C4–In3–C19 105.81(15).

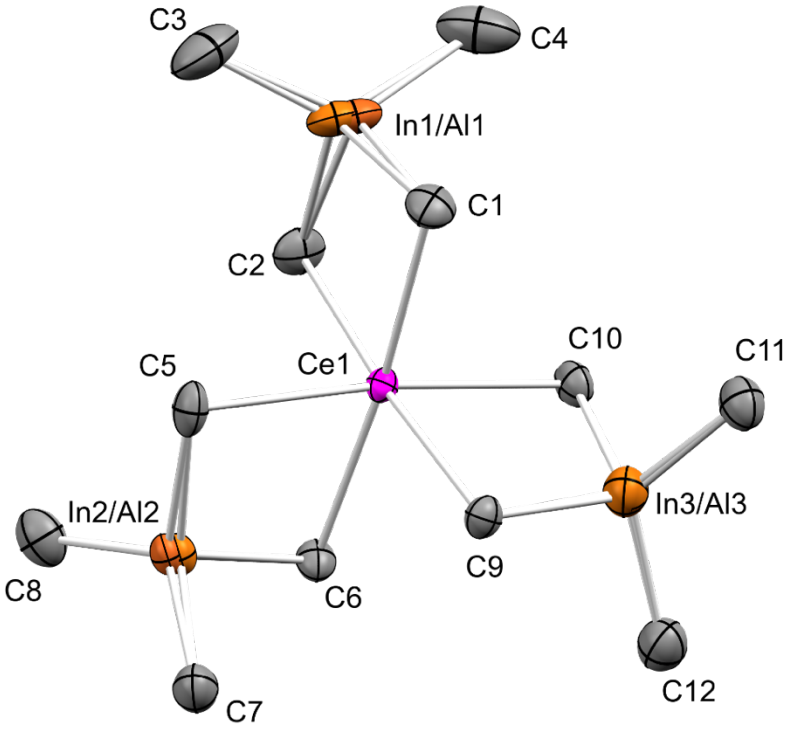

Figure S25. Crystal structure of **6**, with atomic displacement parameters set at 50%. Hydrogen atoms and co-crystallizing $InMe_3$ have been omitted for clarity. Selected interatomic distances (Å) and angles (°): Ce1–C1 2.629(2), Ce1–C2 2.614(3), Ce1–C5 2.649(3), Ce1–C6 2.629(2), Ce1–C9 2.641(2), Ce1–C10 2.632(2), In1–C1 2.241(2), In1–C2 2.270(3), In1–C3 2.102(4), In1–C4 2.052(4), Ce1---In1 3.2836(9), Ce1---In2 3.318(3), Ce1---In3 3.3157(18); C1–Ce1–C2 86.25(8), C1–Ce1–C5 92.29(8), C1–Ce1–C6 175.00(7), C1–Ce1–C9 93.17(8), C5–Ce1–C6 83.02(9), C1–In1–C2 105.19(9), C1–In1–C4 107.43(15), C3–In1–C4 126.40(19).

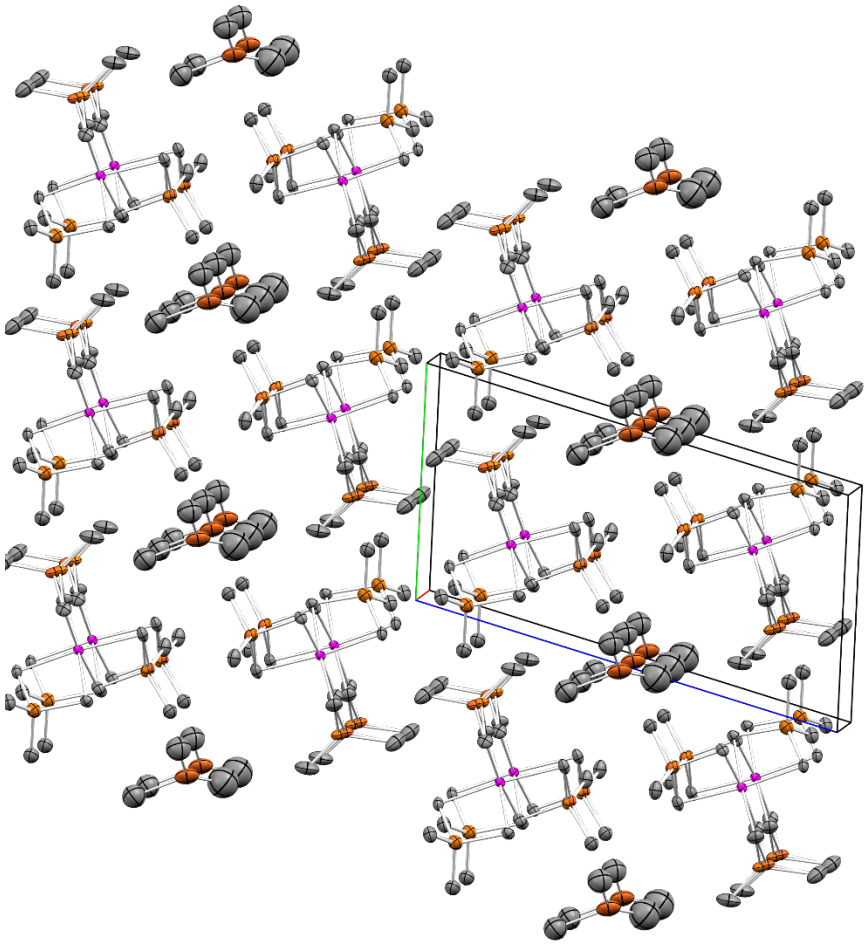

Figure S26. Crystal packing of complex **6**, showing the location of $InMe_3$ in channels formed by $Ce(InMe_4)_3$ molecules.

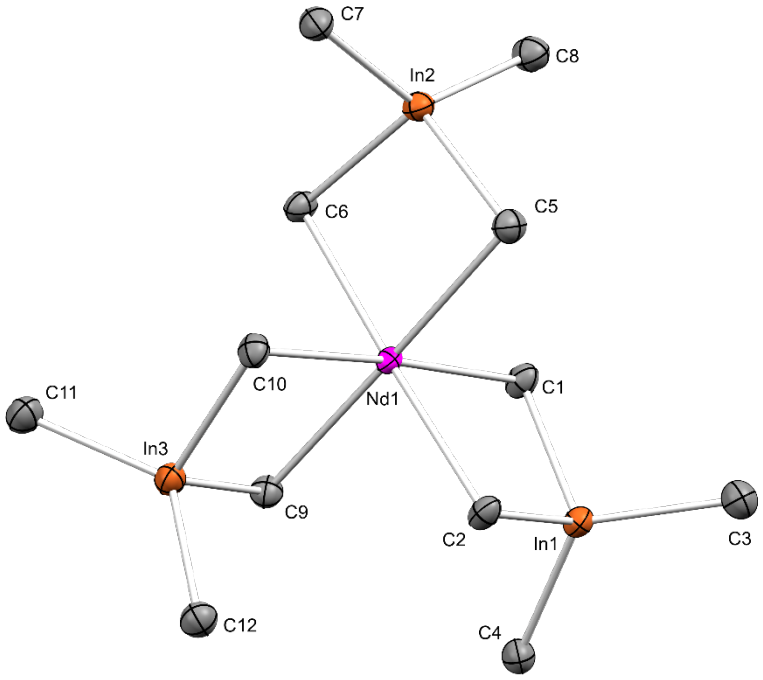

Figure S27. Crystal structure of **7**, with atomic displacement parameters set at 50%. Hydrogen atoms have been omitted for clarity. Selected interatomic distances (Å) and angles (°): Nd1–C1 2.609(3), Nd1–C2 2.626(3), Nd1–C5 2.626(3), Nd1–C6 2.606(3), Nd1–C9 2.622(3), Nd1–C10 2.613(3), In1–C1 2.308(3), In1–C2 2.302(3), In1–C3 2.150(3), In1–C4 2.162(3), Nd1---In1 3.2953(2), Nd1---In2 3.2988(2), Nd1---In3 3.2961(2); C1–Nd1–C2 87.87(9), C1–Nd1–C5 91.54(10), C1–Nd1–C6 90.51(9), C1–Nd1–C9 89.15(9), C5–Nd1–C6 88.88(9), C1–In1–C2 103.98(10), C1–In1–C4 105.63(11), C3–In1–C4 123.75(11).

Table S1. Crystallographic data for compounds **3**, **4a** and **5**

	3	**4a**	**5**
formula	$C_{12}H_{36}In_3La$	$C_{31}H_{71}In_7La_4$	$C_{24}H_{60}InLaN_6$
CCDC	2403536	2403534	2403538
M [g/mol^{-1}]	663.78	1803.25	686.51
colour/shape	colourless/block	colourless/needle	colourless/plate
crystal dimensions [mm]	0.346 x 0.184 x 0.176	0.157 x 0.116 x 0.071	0.215 x 0.120 x 0.086
cryst. System	monoclinic	monoclinic	monoclinic
space group	$P2_1/n$	$P2_1/m$	$P2_1/c$
a [Å]	7.9042(2)	9.1039(7)	8.8745(8)
b [Å]	14.4643(4)	22.1363(17)	21.0266(19)
c [Å]	18.5115(5)	12.8721(10)	17.2739(16)
α [°]	90	90	90
β [°]	94.7640(10)	109.459(2)	100.987(3)
γ [°]	90	90	90
V [Å]	2109.08(10)	2445.9(3)	3164.2(5)
Z	4	2	4
T [K]	100(2)	100(2)	100(2)
wavelength [Å]	0.71073	0.71073	0.71073
P_{caclcd} [Mg/m^{-3}]	2.090	2.448	1.441
μ [mm^{-1}]	5.206	6.657	2.081
F (000)	1248	1656	1408
Θ range [°]	2.208/35.437	2.373/31.682	1.543/30.563
unique reflns	9315	8048	9706
observed reflns	67888	59742	79150
R1[b]/*w*R2(I>2σ)[c]	0.0244/0.0726	0.0386/0.0897	0.0306/0.0726
R1[b]/*w*R2(all data)[c]	0.0263/0.0739	0.0421/0.0912	0.0380/0.0762
GOF[a]	1.087	1.129	1.072

[a]GOF = $[\Sigma w(F_0^2 - F_c^2)^2/(n_0-n_p)]^{1/2}$. [b]$R_1 = \Sigma(|F_0| - |F_c|) / \Sigma |F_0|$, $F_0>4\sigma(F_0)$. [c]$wR_2 = \{\Sigma[w(F_0^2 - F_c^2)^2/ \Sigma[w(F_0^2)^2]\}^{1/2}$.

Table S2. Crystallographic data for compounds **4b**, **6** and **8**

	4b	**6**	**8**
formula	$C_{30}H_{78}In_9La_5$	$C_{12}H_{36}Al_{1.50}CeIn_{1.51}$ •$In(CH_3)_3$	$C_{23}H_{63}Al_{0.39}Ce_3In_{3.61}O$ •1/2 C_7H_8
CCDC	2403535	2403533	2403537
M [g/mol^{-1}]	2166.85	613.63	1246.74
colour/shape	orange/needle	colourless/block	yellow/needle
crystal dimensions [mm]	0.092 x 0.102 x 0.090	0.355 x 0.232 x 0.140	0.282 x 0.058 x 0.024
cryst. System	monoclinic	triclinic	triclinic
space group	C2/c	$P\bar{1}$	$P\bar{1}$
a [Å]	21.745(3)	7.3339(3)	13.1154(5)
b [Å]	12.5180(16)	10.2240(4)	13.3027(5)
c [Å]	23.970(3)	17.7791(7)	14.6787(6)
α [°]	90	102.3840(10)	68.5180(10)
β [°]	102.265(2)	90.3130(10)	86.7520(10)
γ [°]	90	107.7340(10)	61.5310(10)
V [Å]	6375.8(14)	1236.62(9)	2073.04(14)
Z	4	2	2
T [K]	100(2)	100(2)	100(2)
wavelength [Å]	0.71073	0.71073	0.71073
P_{caclcd} [Mg/m^{-3}]	2.257	1.648	1.997
μ [mm^{-1}]	6.466	3.705	5.216
F (000)	3936	594	1180
Θ range [°]	1.888/30.522	2.147/30.519	1.856/28.689
unique reflns	9723	7560	10663
observed reflns	71587	47233	90601
R1[b]/*w*R2(I>2σ)[c]	0.0639/0.1887	0.0242/0.0561	0.0321/0.0745
R1[b]/*w*R2(all data)[c]	0.0692/0.1952	0.0256/0.0572	0.0398/0.0800
GOF[a]	1.046	1.073	1.082

[a]GOF = $[\Sigma w(F_0^2 - F_c^2)^2/(n_0-n_p)]^{1/2}$. [b]$R_1 = \Sigma(|F_0| - |F_c|) / \Sigma |F_0|$, $F_0>4\sigma(F_0)$. [c]$wR_2 = \{\Sigma[w(F_0^2 - F_c^2)^2/ \Sigma[w(F_0^2)^2]\}^{1/2}$.

Table S3. Crystallographic data for compound **7**

	7
formula	$C_{12}H_{36}In_3Nd$
CCDC	2403539
M [g/mol^{-1}]	669.11
colour/shape	colourless/plate
crystal dimensions [mm]	0.217x0.122x0.079
cryst. System	triclinic
space group	$P\overline{1}$
a [Å]	7.8517(2)
b [Å]	10.5549(2)
c [Å]	13.0590(3)
α [°]	87.5080(10)
β [°]	78.9700(10)
γ [°]	77.2910(10)
V [Å]	1036.23(4)
Z	2
T [K]	100(2)
wavelength [Å]	0.71073
P_{caclcd} [Mg/m^{-3}]	2.144
μ [mm^{-1}]	5.742
F (000)	630
Θ range [°]	1.589/30.566
unique reflns	6341
observed reflns	49798
R1[b]/*w*R2(I>2σ)[c]	0.0199/0.0521
R1[b]/*w*R2(all data)[c]	0.0219/0.0533
GOF[a]	1.045

[a]GOF = $[\Sigma w(F_0^2 - F_c^2)^2/(n_0-n_p)]^{1/2}$. [b]$R_1 = \Sigma(|F_0| - |F_c|) / \Sigma |F_0|$, $F_0>4\sigma(F_0)$. [c]$wR_2 = \{\Sigma[w(F_0^2 - F_c^2)^2/\Sigma[w(F_0^2)^2]]\}^{1/2}$.

References

[1] a) A. Fischbach, M. G. Klimpel, M. Widenmeyer, E. Herdtweck, W. Scherer and R. Anwander, *Angew. Chem.*, 2004, **116**, 2284-2289; b) M. Zimmermann, N. Å. Frøystein, A. Fischbach, P. Sirsch, H. M. Dietrich, K. W. Törnroos, E. Herdtweck and R. Anwander, *Chem. Eur. J.*, 2007, **13**, 8784-8800.

[2] COSMO v. 1.61, Bruker AXS Inc., Madison, WI, 2012.

[3] APEX3 V. 2019.11-0, Bruker AXS Inc., Madison, WI, 2019.

[4] SAINT V. 8.40B, Bruker Nano Inc., 2019.

[5] L. Krause, R. Herbst-Irmer, G. M. Sheldrick, and D. Stalke, *J. Appl. Crystallogr.*, 2015, **48**, 3-10.

[6] G. M. Sheldrick, *Acta Crystallogr. Sect. C.*, 2015, **71**, 3-8.

[7] C. B. Hübschle, G. M. Sheldric and B. Dittrich, *J. Appl. Crystallogr.*, 2011, **44**, 1281-1284.

[8] D. Kratzert, J. J. Holstein and I. Krossing, *J. Appl. Crystallogr.*, 2015, **48**, 933-938.

[9] C. F. Macrae, P. R. Edgington, P. McCabe, E. Pidcock, G. P. Shields, R. Taylor, M. Towler and J. v. d. Streek, *J. Appl. Crystallogr.*, 2006, **39**, 453-457.

[10] POV-Ray v.3.6, Persistence of Vision PTy. Ltd., P.-R. Wiliamstown, Victoria, Australia, http://www.povray.org, 2004.